Journal of Engineering Physics and Thermophysics, Vol. 71, No. 5, 1998

CALCULATION OF DETACHED FLOW ALONG A PROFILE OF INTRICATE SHAPE IN THE PRESENCE OF A MOBILE SHIELD BASED ON THE USE OF N-SHAPED ORTHOGONAL GRIDS

S. Ya. Grabarnik and S. A. Isaev

UDC 532.517.2:4

Based on the concept of splitting by physical processes and the use of N-shaped orthogonal grids the authors synthesize a computational algorithm for numerical modeling of detached incompressible viscous flow along a two-dimensional body of intricate shape in the presence of a mobile shield.

1. Development of multiprofile software for numerical modeling of plane flow along bodies of intricate shape, including bodies near a mobile shield, is a complex problem. Its components are synthesis of a finite-volume algorithm based on the concept of splitting by physical processes, construction of a rational grid structure on the basis of choosing the topology of near-orthogonal computational grids, and thorough testing of the created computational system in solving a set of now-classical problems of laminar incompressible viscous flow across a cylinder and turbulent flow along a two-dimensional profile of a Volkswagen automobile. The quest for ensuring the versatility of a software tool when bodies of arbitrary geometry with a rather narrow clearance between them and a mobile wall are considered has motivated the choice of N-grids. That is the reason that one of the central problems in this work was synthesis of an acceptable efficient algorithm for generating an orthogonal grid of the indicated type and detailed comparative analysis of results of calculations on this kind of grid and calculated data obtained on other grids and by other numerical methods as well as available experimental data on local and integral characteristics of detached flows.

2. The methodology of numerical modeling of two-dimensional uniform incompressible viscous flow along a body of arbitrary geometry is based on solving, within the framework of splitting by physical processes, the initial system of Navier–Stokes equations for a laminar regime of flow and the system of Reynolds equations that is closed using a two-parameter dissipative turbulence model for a turbulent regime of flow [1]. The problem of flow along a body in the presence of a mobile shield is considered in a steady-state formulation with allowance for separation of the flow in a wide Reynolds-number range. The turbulent character of flow with developed circulation zones for high Reynolds numbers is modeled within the framework of a modified phenomenological approach that is associated with introduction of vortex viscosity and allows for the effect of the curvature of the current lines on the turbulence characteristics, following the concept of Leschziner and Rodi. The use of a high-Reynolds version of the modified model is combined with employment of the Launder and Spalding method of wall functions.

The system of initial equations in divergent form is written in curvilinear coordinates matched with the contour of the body in the flow for increments in dependent variables that include Cartesian velocity components, pressure, and characterics of turbulence (the kigridic energy of turbulent pulsations and the rate of turbulent-energy dissipation). The control differential equations are discretized using the finite-volume method on an N-type orthogonal grid generated on the basis of an elliptical procedure.

The proposed computational model, which is based on the use of the concept of splitting by physical processes in the form of a SIMPLEC pressure-correction procedure, is realized in an aggregate of the computational units that form it. Characteristic features of this iteration algorithm are determination, on the "predictor" step, of the preliminary velocity components for "frozen" pressure fields and turbulence characteristics and pressure

Academy of Civil Aviation, St. Petersburg. Translated from Inzhenerno-Fizicheskii Zhurnal, Vol. 71, No. 5, pp. 872-879, September-October, 1998. Original article submitted December 16, 1996.

 1062-0125/98/7105-0858$20.00

correction on the basis of solving the continuity equation with subsequent velocity-field corrections and calculation of the characteristics of turbulence and vortex viscosity.

The choice of a centered pattern with tying of dependent variables to the center of a computational cell is dictated by the quest for simplification of the computational algorithm and reduction of the number of computational operations. Pressure-field monotonization, required in this approach, is effected on the basis of the Rhi-Chou methodology [1].

High stability of the computational procedure is ensured by using, for discretization of the convective terms of the equations in the implicit side, one-sided counterflow differences, by damping nonphysical oscillations by introduction of artificial diffusion, and by employing pseudotime stabilizing terms. The method of incomplete matrix factorization for solving the system of nonlinear algebraic equations improves the computational efficiency of the computational algorithm, too. The acceptable accuracy of the procedure is determined by discretization of the explicit side of the equations by the scheme of the second order of approximation, including the convective terms of the equations by Leonard's quadratic counterflow scheme. This methodology makes it possible to minimize the influence of "numerical"-diffusion effects, which are especially substantial when detached flows are calculated.

This efficient computational technology was evaluated on a set of various test problems, including problems that have experimental analogs. Included in the solved problems were well-known problems of circulation motion of a liquid in a cavity and of turbulent detached flow in a channel with a sudden divergence, problems of external flow along bodies of various geometry: longitudinal and transverse cylinders, a sphere, a composition of a disk and a cylinder, etc. It should be noted that, in all the enumerated cases, use was made of canonical grid structures (Cartesian or polar grids). The concept of construction, structure, and characteristic features of the developed computational codes turn out to be comparable to similar characteristics of well-known packages of applied programs: PHOENICS, FLOW3D, FIRE, and others. An important advantage of the developed strategy is its generalization to the case of three-dimensional turbulent flows [2].

3. Let us consider in greater detail the problem of generation of orthogonal computational grids. An orthogonal coordinate system, as is known, can be obtained from the solution of Laplace's equations [3], which, in the transformed plane, have the form

$$\frac{\partial}{\partial \xi}\left(\frac{h_2}{h_1}\frac{\partial f}{\partial \xi}\right) + \frac{\partial}{\partial \eta}\left(\frac{h_1}{h_2}\frac{\partial f}{\partial \eta}\right) = 0\,, \quad f = x, y\,. \tag{1}$$

Boundary conditions that ensure orthogonality at the boundaries of the calculation domain are represented as

$$(\mathbf{r}_\xi \cdot \mathbf{r}_\eta)\,|_\Gamma = 0\,, \tag{2}$$

where r is the position vector.

The grid generator, in addition to the problem of finding the coordinates of the grid nodes proper, solves the problem of controlling the coordinate lines, too. Here we indicate two variants of the solution of this problem.

In the first variant, changes are introduced in the formulation of the boundary conditions. Thus, boundary conditions (2) are stated only at two adjacent boundaries and are fixed at two other boundaries, i.e.,

$$f(\eta) = f_{\Gamma_1}\,, \quad f(\xi) = f_{\Gamma_2}\,; \tag{3a}$$

$$(\mathbf{r}_\xi \cdot \mathbf{r}_\eta)\,|_{\Gamma_3} = 0\,, \quad (\mathbf{r}_\xi \cdot \mathbf{r}_\eta)\,|_{\Gamma_4} = 0\,. \tag{3b}$$

It can be shown that, in this case, the orthogonality condition $\mathbf{r}_\xi \cdot \mathbf{r}_\eta = 0$ will be satisfied both within the calculation domain and at the boundaries Γ_1 and Γ_2. This method of control enables us to draw coordinate lines through prescribed points on the two adjacent boundaries. On the other two boundaries, the coordinates of the nodes are calculated from condition (3b).

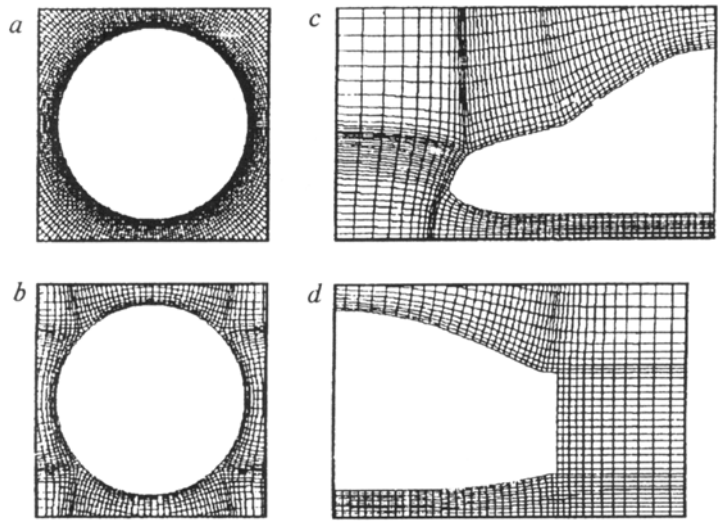

Fig. 1. Fragments of O- and N-type orthogonal computational grids near a cylinder (a, b) and a profile of intricate geometry near a mobile shield (the leading part of the profile (c) and the trailing part of the profile (d)).

Another approach is associated with prescribing preliminary conditions when differential equation (1) is solved. In this case, the position of the coordinate lines can be controlled using the step of the grid in the curvilinear coordinates $\Delta\xi_i$ and $\Delta\eta_j$ and the distribution of the Lamé coefficients. In many works (for example, [4, 5]), the step of the grid is assumed to be constant and equal to unity, and different approximations for the control function $h_1/h_2 = f(\xi, \eta)$ are introduced. But since this function itself is determined in terms of dependent variables, it cannot be prescribed in advance without extending the system of calculation equations.

Therefore, in the present work, a different method of control is chosen within the framework of this approach. Thus, the quantity h_1/h_2 is assumed to be constant in the entire calculation domain. To find it, we employ a Cauchy–Riemann-type condition in the form

$$\frac{1}{h_1}\frac{\partial x}{\partial \xi} = \frac{1}{h_2}\frac{\partial y}{\partial \eta}; \quad \frac{1}{h_1}\frac{\partial y}{\partial \xi} = -\frac{1}{h_2}\frac{\partial x}{\partial \eta},$$

from which the following calculation expression is constructed:

$$\frac{h_2}{h_1} = H = \frac{1}{j_{\max}} \sum_{j=1}^{j=j_{\max}} \frac{\int (x_\eta^2 + y_\eta^2)\, d\xi}{\int (x_\xi^2 + y_\xi^2)\, d\xi}. \tag{4}$$

The system of equations (1) and (4) with boundary conditions (2) is solved numerically by the method of longitudinal-transverse running. A finite-difference analog of differential equation (1) is obtained by the reference-volume method on a five-point grid pattern.

As a result we have

$$a_P f_P = a_E f_E + a_W f_W + a_N f_N + a_S f_S, \quad f = x, y, \tag{5}$$

where

$$a_E = \left(\frac{\Delta\eta}{\delta\xi}\frac{h_2}{h_1}\right)_E, \quad a_W = \left(\frac{\Delta\eta}{\delta\xi}\frac{h_2}{h_1}\right)_W, \quad a_N = \left(\frac{\Delta\xi}{\delta\eta}\frac{h_1}{h_2}\right)_N, \quad a_S = \left(\frac{\Delta\xi}{\delta\eta}\frac{h_1}{h_2}\right)_S,$$

$$a_P = a_E + a_W + a_N + a_S.$$

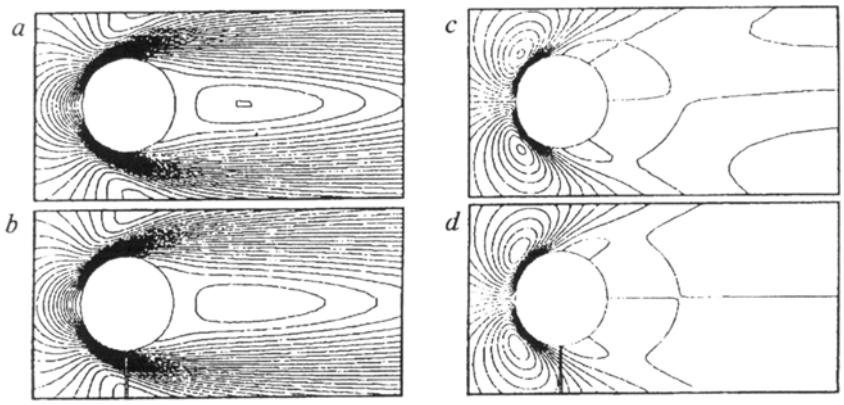

Fig. 2. Comparison of isotach patterns of the longitudinal u (a, b) and transverse v (c, d) velocity components for incompressible viscous flow across a cylinder at Re = 40, calculated on N- (a, c) and O-type (b, d) grids: a, b) the lines are drawn with a step of 0.05 from −0.1 to 1.15; c, d) the same, from −0.55 to 0.55.

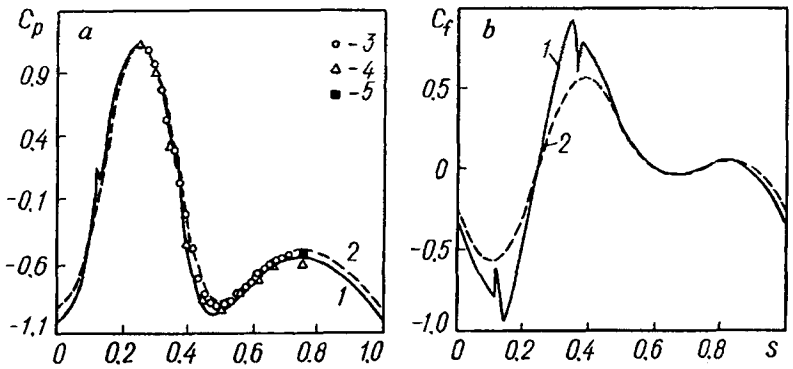

Fig. 3. Comparison of distributions of the pressure C_p (a) and friction C_f (b) factors over the surface of a cylinder in a uniform incompressible viscous flow at Re = 40: 1 and 2) calculated results of this work, N- and O-type grids, respectively; 3 and 4) calculated results of Kawaguti and experimental results of Toma [9]; 5) interval of experimental values of the bottom-pressure coefficient [10].

The computational procedure consists of two steps. In the first step, we find the coordinates of the internal points from finite-difference relations (5). The position of the nodes on the boundary is taken from the previous iteration. Next, the coordinates of the boundary nodes are calculated from condition (2).

Figure 1b presents a fragment of an orthogonal grid around a circular cylinder. Here, a combined method of control is realized. On the internal contour, four critical points that divide the entire calculation domain into eight subdomains are fixed. In each subdomain, its own value of h_1/h_2 is calculated, which is subsequently used in determining the coefficients of Eq. (5). Within the limits of a subdomain, its own distribution law for the steps of the grid is prescribed, which is determined in a numerical experiment from the condition of an appropriate degree of bunching of the step of the grid at the surface of the body in the flow.

4. The methodological part of the investigation contains a comparative analysis of results of calculations of laminar incompressible viscous flow across a cylinder for a Reynolds number Re = 40, performed on grids of different types by the presented procedure, and available calculated and experimental data [6-10]. The cylinder diameter is chosen as the characteristic dimension, and the incoming-flow velocity is taken as the velocity scale. See Figs. 2 and 3 and Table 1 for materials of the analysis.

Numerical modeling of detached flow across a cylinder is performed on an O-type analytical grid that contains 60 × 220 computational cells, distributed with bunching toward the cylinder surface, and on elliptical

TABLE 1. Comparison of Calculated Results for Laminar Incompressible Viscous Flow along a Cylinder at a Reynolds Number Re = 40

No. of column*)	1	2	3	4	5
Type of grid	N-type		O-type		
Number of cells	93 × 93	121 × 121	60 × 220	62 × 100	3000–4000
C_{xp}	0.406	0.387	0.398	–	–
C_{xd}	0.606	0.596	0.583	–	–
$C_{xp} + C_{xd}$	1.012	0.983	0.981	0.981	0.976
C_{xf}	0.642	0.659	0.517	0.5163	0.549
C_x	1.653	1.642	1.498	1.497	1.5025
C_{pf}	1.139	1.109	1.146	1.13	–
C_{pd}	−0.500	−0.488	−0.473	−0.484	–
X_s	2.237	2.075	2.23	2.33	–

*)In columns 1-3, there are results of the present work, and in 4 and 5 the data are taken from [6] and [7], respectively.

TABLE 2. Calculated Results for Integral Characteristics of Turbulent Flow along a Two-Dimensional Model of a Volkswagen Automobile at a Reynolds Number Re = 10^7

C_{xp}	C_{xd}	C_{xf}	C_x	C_{xn}	u_{min}	k_{max}	X_s
−0.022	0.099	0.0099	0.087	−0.139	−0.106	0.0588	0.449

N-type grids that are constructed by the described procedure and contain 93 × 93 and 121 × 121 computational cells. Fragments of the indicated grids are given in Fig. 1.

As follows from a comparison of the fields of local characteristics of flow across a cylinder (Fig. 2) the flow patterns obtained in calculations on rather detailed grids of different types are practically the same. Nonetheless, the surface distributions of the pressure and friction factors (Fig. 3) reveal differences in the character of the curves due to the topological features of the N-type curvilinear grid. These differences, naturally, are more pronounced in the behavior of the factor C_f, where quantitative discrepancies are noticeable for the chosen Reynolds number. For local force loads, the pressure spike of circuit origin is very small in length and magnitude. Therefore its contribution to the imbalance of the integral force load turns out to be extremely insignificant.

The obtained calculated results on C_p are in very close agreement with each other and with results of Kawaguti's calculation and Toma's experimental data on the portion of accelerating and retarded flows near the cylinder. These is disagreement only in the bottom region. However, the more detailed experimental data of Williamson and Roshko [8] provide an idea of the existing spread in the results of measurements, in which the obtained calculated characteristics fit.

Data for integral characteristics of flow across a cylinder calculated with the use of various algorithms and grids are summarized in Table 1. For comparison, we give results obtained on the basis of solving Navier–Stokes equations that are written in transformed variables (vorticity–current function). In [6], a finite-difference algorithm is synthesized using Arakawa's scheme of the second and fourth order of approximation. Consideration was given to a very detailed computational grid that contained 62 × 100 nodes. An earlier work [7] was performed on the basis of employing central finite differences, and the chosen number of computational nodes of the grid was quite large (3000–4000). In addition to the given results, we should note that, according to Apelt's experimenttal data from monograph [9], for Re = 40, C_x = 1.513, while, according to the experimental data of [10], the length of the circulation zone behind the cylinder is X_s = 2.2.

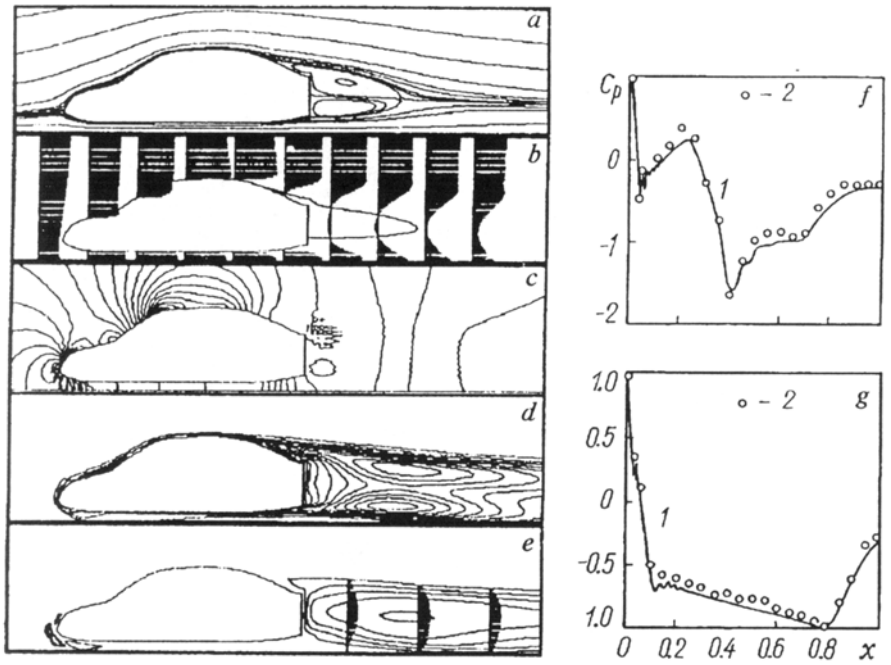

Fig. 4. Field patterns (a-e) of the characteristics of turbulent flow along a profile of intricate geometry near a mobile shield for $Re = 10^7$ and comparison of calculated and experimental distributions of the static-pressure coefficient C_p along the chord of the profile: a) current lines that correspond to the values of the current functions: −0.03, −0.01, −0.05, −0.001, 0, 0.001, 0.005, 0.01, 0.03, 0.1, 0.2, 0.3; b) profiles of the longitudinal velocity component; c) isobars with a 0.05 step from −0.75 to 0.5; d) pattern of isolines of the turbulent-pulsation kigridic energy k, drawn with a 0.005 step from 0.005 to 0.05; e) the same, for the vortex viscosity ν_t, drawn with a 0.0005 step from a background value of 0.0015 to 0.0025; the calculated values of C_p, constructed along the chord (curves 1 in Fig. 4f and g), refer to the upper and lower sides of the profile, respectively; the experimental data (points 2) for the comparison are taken from [11, 12].

From consideration of the data of Table 1 and the distributions of the pressure factor C_p in Fig. 3a it follows that all the integral or local characteristics presented, except for the friction resistance C_{xf}, are in good agreement with each other and with the available experimental data. This means that the results of numerical modeling of laminar flow across a cylinder depend weakly on the type of computational grid. At the same time, we cannot but note the effect of the topology of the grid on the distribution of the surface friction factor, which causes an over estimation (up to 10%) of the friction resistance.

5. Some results of calculation of turbulent steady flow along a profile of intricate geometry that is a two-dimensional model of a Volkswagen automobile in the vicinity of a mobile shield for $Re = 10^7$ are summed up in Fig. 4 and Table 2. To solve the problem of two-dimensional flow along the outline of the automobile, we chose a near-orthogonal N-type grid (with a rectangular cut at the center of a curvilinear calculation domain). Figure 1c and d presents fragments of the grid in the front (c) and rear (d) parts of the automobile. The calculation domain is divided into 150 × 60 nonuniformly distributed cells. The automobile outline accounts for 15 cells in the transverse direction and 81 cells in the longitudinal direction. The entrance boundary is prescribed at a distance of 7.5 of the chord of the automobile profile, chosen as the characteristic dimension in this problem. The exit boundary is located at a distance of 5.6 from the profile. The vertical dimension of the calculation domain is 3.39. The clearance is 0.06. The thickness of the automobile profile is 0.3. A uniform flow that models flow in the working portion of a subsonic wind tunnel is prescribed at the entrance boundary; "mild" boundary conditions are stated

at the upper and exit boundaries while conditions that correspond to the mobile shield are prescribed at the lower boundary, i.e., the solid wall moves with the velocity of the incoming flow.

From the patterns of developed turbulent flow along the profile presented in Fig. 4a-e it can be seen that the detached flow in the near wake has the structure of two large-scale vortices. The velocity of the return flow in the wake turns out to be of the order of 0.1. The separation point of the flow, similarly to [11], is located on the diffuser upper part of the outline, and the velocities in the separation zone adjacent to the windshield are very small. Examination of the velocity profiles in the near wake points to the occurrence of a jet flow in the direction toward the automobile with its subsequent spreading over the frame.

The dimensions of the separation zone behind the automobile are comparatively small and are of the order of 0.45 in the longitudinal direction. The velocity profile in the wake behind the body has a characteristic minimum; here, two shear flows develop: a wall jet near the mobile shield and detached shear flow in a curvilinear channel behind the backward step. No separation of the flow at the mobile shield behind the profile, similarly to what was shown in [11], was detected. The pressure field has a strong inhomogeneity in the upper part of the outline with a pronounced rarefaction in the convex part. The zone of increased pressure is correctly reproduced in front of the concavity in the vicinity of the windshield. A very thin and nonextended separation zone forms there. In the gap between the automobile and the shield, a channel-type accelerating flow with a pressure drop along the channel length is realized. The wake region, conversely, is characterized by the isobaricity that is inherent in jet flows. The field of the kigridic turbulence energy has two zones of maxima in the wake behind the automobile that are located in shear regions of the flow. At the same time, the vortex viscosity is maximum at the center of the jet that acts on the rear part of the automobile.

Figure 4f and g compares calculated profiles of the pressure factor C_p on the upper and lower sides of the outline with experimental data taken from [11, 12]. The very close agreement of the results presented indicates the acceptability of the developed system for engineering practice. Attention is drawn to the fact that the profile resistance of the body turns out to be negative while the normal force presses it against the mobile shield.

The authors express their thanks to Professor A. S. Ginevskii for useful discussions of the problem.

The work was carried out with financial support from the Russian Fund for Fundamental Research, project No. 96-01-01290.

NOTATION

x and y, longitudinal and transverse Cartesian coordinates; ξ and η, transformed curvilinear coordinates matched with the outline of the body in the flow; h_1 and h_2, Lamé coefficients; s, relative distance along the outline of the body; $\Delta\xi$ and $\Delta\eta$, dimensions of the computational cell in curvilinear coordinates; $\delta\xi$ and $\delta\eta$, distances between the nodes of the computational grid in the ξ and η directions, respectively; u and v, Cartesian velocity components; ρ and p, density of the fluid and excess pressure referred to the doubled velocity head; k and ε, energy of turbulent pulsations and its dissipation rate; ν, kinematic-viscosity factor of the fluid; C_p, pressure factor; C_f, friction factor; Re, Reynolds number; ψ, current function; C_x, C_{xp}, C_{xd}, C_{xf}, and C_{xn}, drag coefficient, coefficients of profile, bottom, and frictional resistance, and coefficient of normal force; X_s, length of the separation zone in the near wake behind the body. Subscripts: i and j, numbers of the grid lines; t, turbulent; f, parameter at the leading critical point of the body; d, parameter in the bottom region behind the body; max and min, maximum and minimum.

REFERENCES

1. I. A. Belov, S. A. Isaev, and V. A. Korobkov, Problems and Methods of Calculation of Detached Flows of an Incompressible Fluid [in Russian], Leningrad (1989).
2. S. A. Isaev, V. B. Kharchenko, and Ya. P. Chudnovskii, Inzh.-Fiz. Zh., 67, Nos. 5-6, 1013-1017 (1994).
3. J. F. Thompson, Z. U. Warsi, and C. W. Mastin, Numerical Grid Generation. Foundations and Applications, North-Holland, New York (1985).

4. M. R. Albert, Numerical Grid Generation in Computational Fluid Mechanics '88, Mumbles (1988), pp. 425-433.
5. A. A. Rangvalla and B. R. Munson, J. Computational Physics, 70, 373-396 (1987).
6. I. A. Belov and N. A. Kudryavtsev, Heat Transfer and Resistance of Tube Banks [in Russian], Leningrad (1986).
7. A. E. Hamielec and J. D. Raal, Phys. Fluids, 12, No. 1, 10-12 (1969).
8. C. H. Williamson and A. Roshko, Z. Flügwiss. Weltraumforsch., 14, 38 (1990).
9. J. Batchelor, Dynamics of an Incompressible Viscous Fluid [Russian translation], Moscow (1973).
10. M. Coutanceau and R. Bouard, J. Fluid Mech., 79, Part 2, 231-256 (1977).
11. R. Buchheim, H. Röhe, and H. Wüsteberg, Volkswagen. Forschung-neue technologien. Sonderdruck aus ATZ Automobijtechnische Zeitschrift, No. 91 (1989).
12. K. Kitoh, T. Kobayashi, and H. Morooka, Comput. Mech. 86: Theory and Appl., Proc. Int. Conf., Tokyo (1986), pp. 77-82.